Acta Crystallographica Section C
Crystal Structure Communications
ISSN 0108-2701

Multicomponent crystals of erlotinib

B. Sridhar,[a]* K. Ravikumar,[a] Harihara Krishnan[b] and A. N. Singh[b]

[a]Laboratory of X-ray Crystallography, Indian Institute of Chemical Technology, Hyderabad 500 007, India, and [b]SMS Pharma Research Centre, Hyderabad 500 038, India
Correspondence e-mail: sshiya@yahoo.com

Received 7 October 2009
Accepted 7 December 2009
Online 19 December 2009

Erlotinib [systematic name: *N*-(3-ethynylphenyl)-6,7-bis(2-methoxyethoxy)quinazolin-4-amine], a small-molecule epidermal growth factor receptor inhibitor, useful for the treatment of non-small-cell lung cancer, has been crystallized as erlotinib monohydrate, $C_{22}H_{23}N_3O_4\cdot H_2O$, (I), the erlotinib hemioxalate salt [systematic name: 4-amino-*N*-(3-ethynylphenyl)-6,7-bis-(2-methoxyethoxy)quinazolin-1-ium hemioxalate], $C_{22}H_{24}N_3O_4^{+}\cdot 0.5C_2O_4^{2-}$, (II), and the cocrystal erlotinib fumaric acid hemisolvate dihydrate, $C_{22}H_{23}N_3O_4\cdot 0.5C_4H_4O_4\cdot 2H_2O$, (III). In (II) and (III), the oxalate anion and the fumaric acid molecule are located across inversion centres. The water molecules in (I) and (III) play an active role in hydrogen-bonding interactions which lead to the formation of tetrameric and hexameric hydrogen-bonded networks, while in (II) the cations and anions form a tetrameric hydrogen-bonded network in the crystal packing. The title multicomponent crystals of erlotinib have been elucidated to study the assembly of molecules through intermolecular interactions, such as hydrogen bonds and aromatic π–π stacking.

Comment

Understanding the various types and strengths of noncovalent interactions that bind molecules in crystal structures is very important for molecular recognition in chemical and complex biological processes (Glusker, 1998). These studies are significant because of their application in crystal engineering, supramolecular chemistry and the design of functional materials and drugs (Desiraju & Steiner, 1999). In this context, the multicomponent crystals of the drug molecule of erlotinib were grown. Erlotinib is a small-molecule epidermal growth factor receptor (EGFR) tyrosine kinase inhibitor (Rusch *et al.*, 1996). EGFR is a protein tyrosine kinase that plays a crucial role in signal transduction pathways which regulate key cellular functions such as survival and proliferation. Over-expression of EGFR tyrosine kinase is reported in a variety of human tumours and is associated with poor prognosis (Yarden & Ullrich, 1988). Similar to gefitinib, erlotinib specifically targets the EGFR tyrosine kinase, which is highly expressed and occasionally mutated in various forms of cancer. Gefitinib (Iressa) and erlotinib (Tarceca) are the two clinically used EGFR tyrosine kinase inhibitors that demonstrate significant efficacy in non-small-cell lung cancer, leading to FDA (US Food and Drug Administration) approval for the treatment of this refractory disease. Multicomponent crystals are composed of two or more components associated through intermolecular interactions, and the salts and cocrystals can both be described as multicomponent crystals (Stahly, 2007). Recently, we have reported the crystal structure of erlotinib hydrochloride (Selvanayagam *et al.*, 2008), (IV). In the present study, the crystal structures of erlotinib hydrate, (I), erlotinib hemi-oxalate, (II), and erlotinib hemifumaric acid dihydrate, (III), and their intermolecular interactions which hold the assembly of molecules in the crystalline lattice are presented.

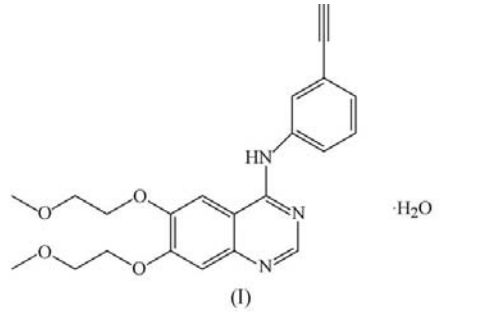

(I)

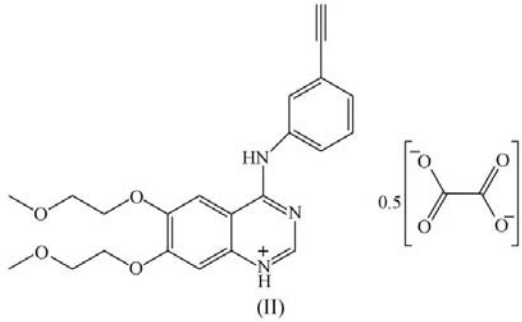

(II)

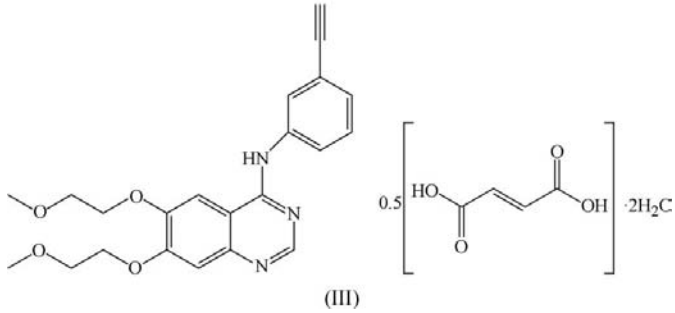

(III)

The asymmetric unit of (I) contains one erlotinib molecule and one water molecule, the asymmetric unit of (II) contains one erlotinib cation protonated at atom N1 and an oxalate dianion lying across an inversion centre, while the asymmetric unit of (III) consists of one erlotinib molecule, a fumaric acid molecule lying across an inversion centre and two water molecules (Figs. 1, 2 and 3). The bond distances and angles of the erlotinib molecules in (I), (II) and (III) are similar and agree well with the values found in related structures (Selva-

 doi:10.1107/S0108270109052470

nayagam *et al.*, 2008; Xia, 2005; Ghosh *et al.*, 2001). In (I), the atoms C13/O2/C14 of the 2-methoxyethoxy side chain are disordered over two sites, with occupancies of 0.554 (7) and 0.446 (7), and in (III) atoms O5/O6/C23/C24 of the hemifumaric acid are disordered over two sites, with occupancies of 0.55 (2) and 0.45 (2).

The inequality of the C—O distances and O—C—C angles (Table 1) confirms the carboxylate group (O5/O6/C23) in (II), while in (III) the near equality of C—O distances and O—C—C angles (Table 1) clearly shows the existence of the carboxyl group (O5/O6/C23). In (III), the O—H bond of the carboxyl group is in *cis* conformation with respect to the C═O bond, as evidenced from the H5*O*—O5—C23—O6 torsion angle of 12.7°.

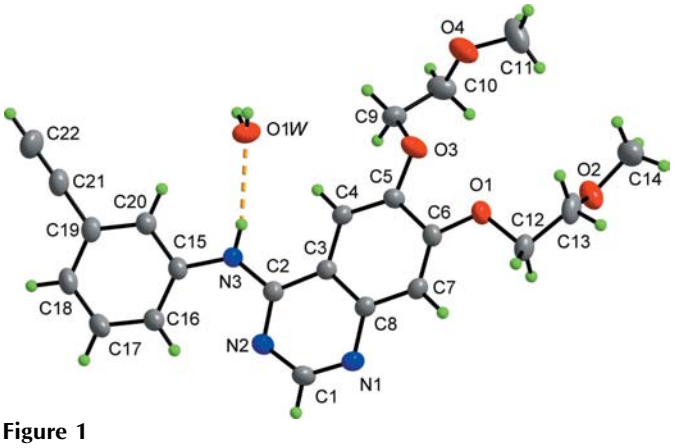

Figure 1
A view of (I), showing the atom-numbering scheme. Displacement ellipsoids are drawn at the 30% probability level and H atoms are shown as small spheres of arbitrary radii. The dashed line indicates a hydrogen bond. The minor components of disordered atoms C131/O21/C141 have been omitted for clarity.

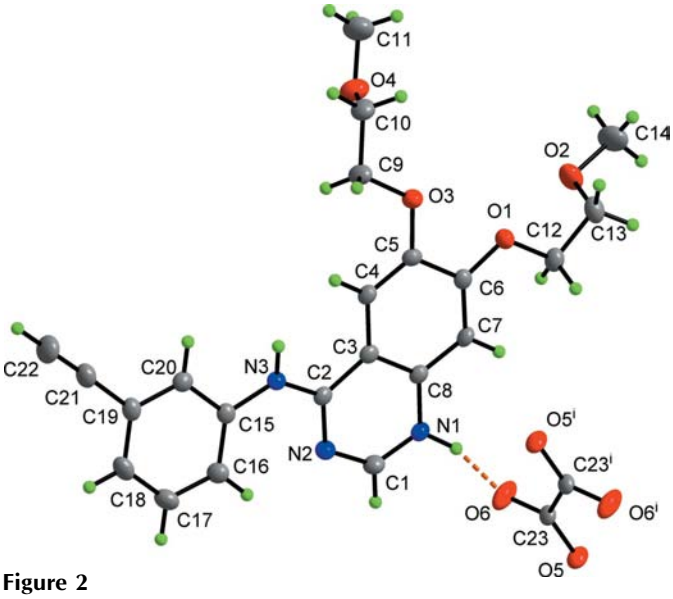

Figure 2
A view of (II), showing the atom-numbering scheme. Displacement ellipsoids are drawn at the 30% probability level and H atoms are shown as small spheres of arbitrary radii. The dashed line indicates a hydrogen bond. [Symmetry code: (i) $-x+2, -y+2, -z$.]

The crystal structure of the erlotinib inhibitor in complex with the EGFR kinase domain, (V) [Stamos *et al.*, 2002; Protein Data Bank (PDB; Berman *et al.*, 2000) entry 1m17] is available and the extracted ligand structure is used for comparison. The torsion angles C3—C2—N3—C15 and C2—N3—C15—C16 define the relative orientation of the quinazoline and ethynylphenyl moieties, respectively. In all three structures [*viz.* (I), (II) and (III)] the two ring systems are relatively close to being coplanar, the dihedral angle between these two ring moieties being 6.2 (1)° for (I), 2.8 (1)° for (II) and 22.8 (1)° for (III). The corresponding interplanar angle between the aromatic ring systems is 42° for (V) and 34.4 (1)° for (IV). However, in (III), and in both (IV) and (V), there is a rotation of the ethynylphenyl ring with respect to the quinazoline ring system.

An overlay of the erlotinib molecules, superimposing the quinazoline ring system, reveals the twist in the ethynylphenyl ring with respect to the quinazoline ring system as well as the relative orientation difference of the two 2-methoxyethoxy side chains (Fig. 4).

The conformation of the 2-methoxyethoxy side chains can be defined from the torsion angles C—O—C—C, O—C—C—O, C—C—O—C and the conformation is *anti–gauche–anti* (*aga*) for both C5 and C6 side chains. The main difference between the two rings and between the three structures is the change of signs in the *anti* and *gauche* conformations. However, in the case of (IV) and (V), a significant difference is observed in the conformation of the

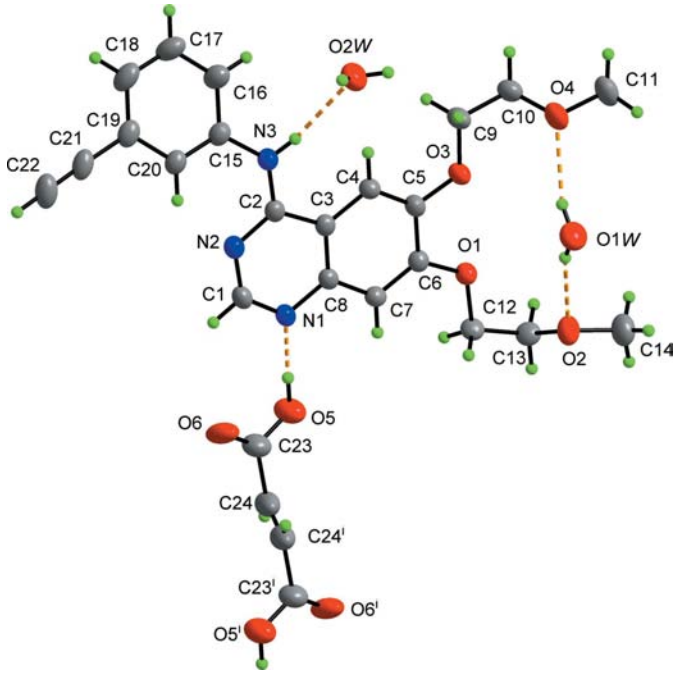

Figure 3
A view of (III), showing the atom-numbering scheme. Displacement ellipsoids are drawn at the 30% probability level and H atoms are shown as small spheres of arbitrary radii. The minor components of disordered atoms O51/O61/C231/C241 of the hemifumaric acid molecule have been omitted for clarity. The dashed lines indicate hydrogen bonds. [Symmetry code: (i) $-x, -y, -z+1$.]

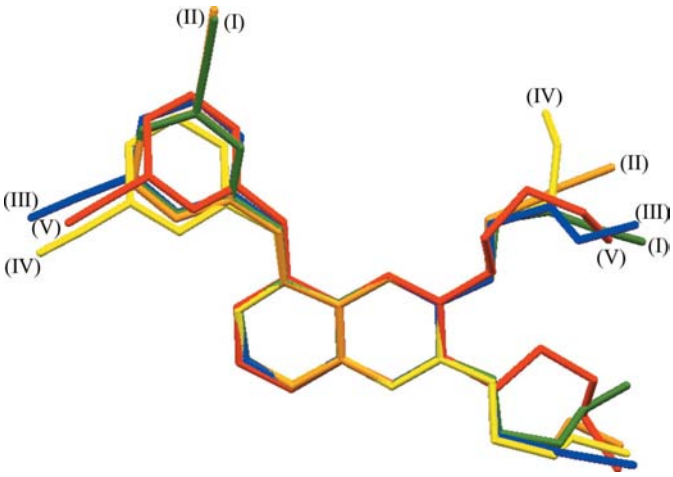

Figure 4
A superposition of the molecular conformations of erlotinib molecules. The overlay was made by making a least-squares fit through the quinazoline ring system of erlotinib–EGFR kinase complex (V). The labels and r.m.s. deviations (Å) are as follows: erlotinib hydrate, (I), 0.076; erlotinib hemioxalate, (II), 0.087; erlotinib hemifumaric acid dihydrate, (III), 0.07; erlotinib HCl, (IV), 0.076.

side chains. The corresponding conformations are found to be (−)*a*–(−)*g*–(+)*g* and (−)*a*–(+)*g*–(−)*a* for (V), (+)*a*–(−)*g*–(−)*a* and (+)*a*–(−)*a*–(−)*g* for (IV).

For convenience, we denote the rings formed by atoms N1–C8 and C3–C8 comprising the quinazoline as rings *A* and *B*, respectively, and atoms C15–C20 of the ethynylphenyl ring as *C*.

In (I) and (III), three types of hydrogen bonds, *viz*. N—H···O, O—H···O and O—H···N, are observed, while in (II), only one type of hydrogen bonding, *viz*. N—H···O, is observed (Tables 2, 3 and 4). In all three structures, hydrogen bonds and aromatic *π*–*π* stacking interactions play a key role in assembling the supramolecular structure.

In (I), the water molecule acts as both donor and acceptor (Table 2). As donor, it forms a hydrogen bond to O3 of the 2-methoxyethoxy side chain and to N1 of the quinazoline ring of a second erlotinib molecule. As acceptor, it links to atom N3 of a third erlotinib molecule. The combination of the first and third of these hydrogen bonds leads to the formation of a centrosymmetric tetramer which may be described in graph-set notation as $R_4^4(18)$ (Etter, 1990; Etter *et al.*, 1990; Bernstein *et al.*, 1995). The $R_4^4(18)$ tetramers are further linked by O—H···N hydrogen bonds, thereby leading to an infinite one-dimensional chain running along the *a* axis (Fig. 5). Intermolecular stacking *via* aromatic *π*–*π* interactions is also present between the *B* and *C* rings [centroid–centroid separation = 3.7381 (9) Å; symmetry code: 1 − *x*, 1 − *y*, 2 − *z*] forming centrosymmetric dimers in (I).

In (II), cation-to-anion N—H···O hydrogen bonds stabilize the crystal structure (Table 3). N1 of the erlotinib cation forms a hydrogen bond to O6 of the oxalate anion, while N3 links to O5 of a translation-related anion. This creates hydrogen-bonded columns along *b* including an $R_4^4(22)$ motif (Fig. 6). Face-to-face stacking interactions between adjacent symmetry-related quinazoline rings *A* and *B* [centroid–centroid separation = 3.7625 (14) Å; symmetry code: 1 − *x*, 1 − *y*, −*z*] and between quinazoline ring *B* and ethynylphenyl ring *C* [centroid–centroid separation = 3.4637 (15) Å; symmetry code: 1 − *x*, 1 − *y*, −*z*] consolidate the supramolecular structure. Propagation of these two *π*-stacking interactions links the molecules into sheets in (II).

In (III), both water molecules play a dual role as donor and acceptor (Table 4). Water molecule O1*W* as donor links the two O atoms of the methoxyethoxy side chains through intramolecular O—H···O hydrogen bonds and so forms an $R_2^2(13)$ motif. In its capacity as donor, the second water molecule, O2*W*, forms hydrogen bonds to O1*W* and to the carbonyl O atom of a fumaric acid molecule. In addition, O2*W* acts as acceptor in a hydrogen bond from N3 of the erlotinib molecule, analogous to the hydrogen bond observed in (I). In the erlotinib–EGFR kinase complex structure, the same N

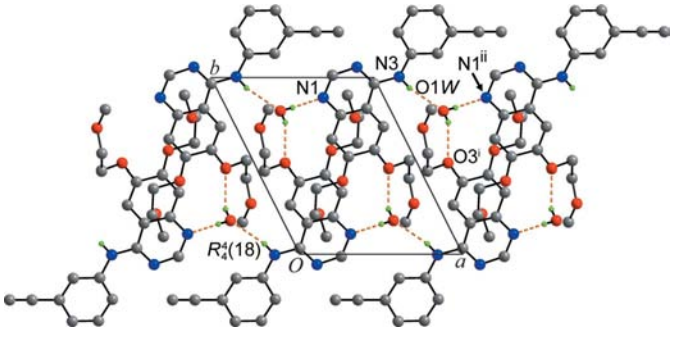

Figure 5
A packing diagram for (I), viewed down the *c* axis, showing the centrosymmetric tetramer $R_4^4(18)$ ring motif. Hydrogen bonds are shown as dashed lines. H atoms not involved in hydrogen bonding and the minor components of disordered atoms C131/O21/C141 have been omitted for clarity. Only atoms involved in hydrogen bonding are labelled. [Symmetry codes: (i) −*x* + 2, −*y* + 1, −*z* + 2; (ii) *x* + 1, *y*, *z*.]

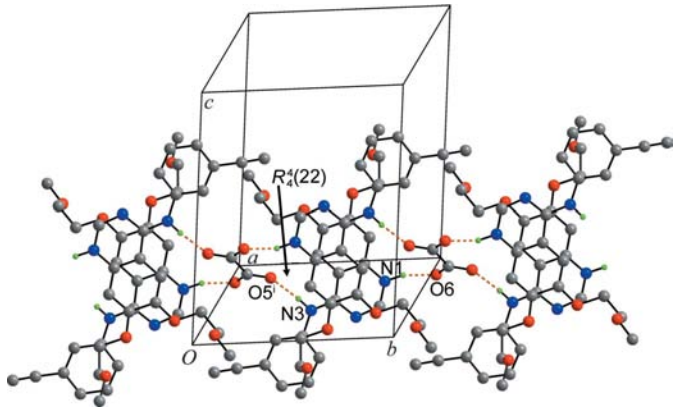

Figure 6
A packing diagram for (II), viewed through the *a* axis, showing centrosymmetric tetrameric [$R_4^4(22)$] hydrogen-bonded columns. Hydrogen bonds are shown as dashed lines and H atoms not involved in hydrogen bonding have been omitted for clarity. Only atoms involved in hydrogen bonding are labelled. [Symmetry code: (i) *x*, *y* − 1, *z*.]

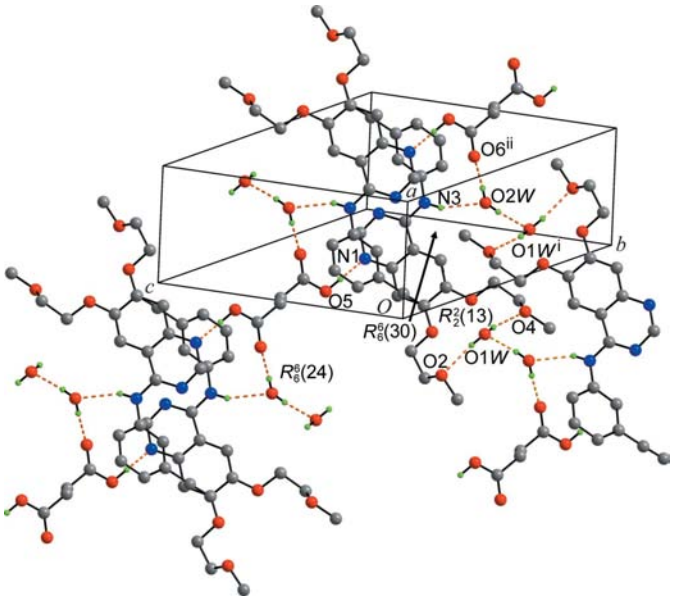

Figure 7
A partial packing view of (III), showing two hexameric [$R_6^6(30)$ and $R_6^6(24)$] hydrogen-bonded networks. Hydrogen bonds are shown as dashed lines and H atoms not involved in hydrogen bonding and the minor components of disordered atoms O51/O61/C231/C241 of the hemifumaric acid molecule have been omitted for clarity. Only atoms involved in hydrogen bonding are labelled. [Symmetry codes: (i) $-x$, $-y+1$, $-z$; (ii) $-x+1$, $-y+1$, $-z+1$.]

atom (N3) is also hydrogen bonded only with the water molecule. Thus, in (III), the water–water linkage interconnects the erlotinib molecules *via* O—H···O and O···H—N hydrogen bonds and leads to the formation of an $R_6^6(30)$ motif. Each $R_6^6(30)$ motif is arranged as a hexameric hydrogen-bonded network consisting of two sets of centrosymmetrically related erlotinib molecules and two sets of water–water linkages (Fig. 7). The fumaric acid lying across the centre of inversion forms a linear hydrogen-bonded trimer through an intramolecular O—H···N hydrogen bond with the two erlotinib molecules. In addition, it forms an O—H···O hydrogen bond with the second water molecule (O2*W*). Thus, the combination of these two O—H···N and O—H···O hydrogen bonds forms another set of hexameric hydrogen-bonded networks of $R_6^6(24)$ motif. The $R_6^6(30)$ and $R_6^6(24)$ motifs are arranged alternately and aggregate as infinite two-dimensional supramolecular hydrogen-bonded networks (Fig. 7).

In (III), pairs of molecules are linked to centrosymmetric dimers similar to (I) by means of two aromatic π–π interactions, *viz*. between ring *A* and its inversion-related ring *A* [centroid–centroid separation = 3.7249 (17) Å; symmetry code: $-x, 1-y, 1-z$], and between ring *A* and ring *B* [centroid–centroid separation = 3.6201 (16) Å; symmetry code: $1-x, 1-y, 1-z$]. In all three structures, weak C—H···O, C—H···N and C—H···π interactions are observed.

Experimental

To obtain crystals of (I) suitable for X-ray study, erlotinib (SMS Pharma Research Centre, Hyderabad) (40 mg) was dissolved in water (10 ml) and the solution allowed to evaporate slowly. Crystals of (II) and (III) were obtained by slow evaporation from a mixture of methanol (5 ml) and water (1 ml) with erlotinib (40 mg) and oxalic acid (10 mg) in (II), and with erlotinib (40 mg) and fumaric acid (120 mg) in (III).

Compound (I)

Crystal data

$C_{22}H_{23}N_3O_4\cdot H_2O$
M_r = 411.45
Triclinic, $P\overline{1}$
a = 9.0227 (10) Å
b = 10.4548 (11) Å
c = 13.2014 (14) Å
α = 98.705 (2)°
β = 108.738 (2)°
γ = 111.873 (2)°
V = 1041.05 (19) Å^3
Z = 2
Mo $K\alpha$ radiation
μ = 0.09 mm^{-1}
T = 294 K
0.19 × 0.13 × 0.09 mm

Data collection

Bruker SMART APEX CCD area-detector diffractometer
10097 measured reflections
3666 independent reflections
3169 reflections with $I > 2\sigma(I)$
R_{int} = 0.017

Refinement

$R[F^2 > 2\sigma(F^2)]$ = 0.043
$wR(F^2)$ = 0.120
S = 1.03
3666 reflections
311 parameters
21 restraints
H atoms treated by a mixture of independent and constrained refinement
$\Delta\rho_{max}$ = 0.18 e Å^{-3}
$\Delta\rho_{min}$ = −0.28 e Å^{-3}

Compound (II)

Crystal data

$C_{22}H_{24}N_3O_4^+\cdot 0.5C_2O_4^{2-}$
M_r = 438.45
Triclinic, $P\overline{1}$
a = 7.6285 (8) Å
b = 10.2252 (10) Å
c = 14.6525 (14) Å
α = 86.076 (2)°
β = 84.925 (2)°
γ = 70.559 (2)°
V = 1072.62 (18) Å^3
Z = 2
Mo $K\alpha$ radiation
μ = 0.10 mm^{-1}
T = 294 K
0.17 × 0.09 × 0.06 mm

Table 1
Selected geometric parameters (Å, °) for (I), (II) and (III).

	(I)	(II)	(III)	(IV)†	(V)‡
C23—O5		1.235 (3)	1.273 (11)		
C23—O6		1.246 (3)	1.214 (11)		
C1—N1	1.308 (2)	1.303 (3)	1.303 (3)	1.317 (3)	1.411
C1—N2	1.346 (2)	1.322 (3)	1.334 (3)	1.309 (3)	1.416
C2—N2	1.330 (2)	1.342 (3)	1.327 (3)	1.353 (3)	1.414
C2—N3	1.365 (2)	1.341 (3)	1.351 (3)	1.337 (3)	1.455
C8—N1	1.379 (2)	1.372 (3)	1.373 (2)	1.378 (3)	1.443
C1—N1—C8	115.4 (1)	119.7 (2)	117.2 (2)	120.4 (2)	119.6
C2—N2—C1	116.8 (1)	117.2 (2)	117.0 (2)	125.4 (2)	120.6
C2—N3—C15	130.3 (1)	130.9 (2)	129.2 (2)	127.4 (2)	134.0
O5—C23—O6		125.2 (2)	122.9 (12)		
O5—C23—C23^i		116.8 (3)			
O6—C23—C23^i		118.0 (3)			
O5—C23—C24§			124.8 (10)		
O6—C23—C24§			112.2 (10)		
C3—C2—N3—C15	−179.2 (1)	−179.7 (2)	167.9 (2)	−178.8 (2)	−174.9
C2—N3—C15—C16	−3.3 (2)	8.2 (4)	−152.9 (2)	−146.2 (2)	−138.4

Symmetry code: (i) $-x+2, -y+2, -z$. † Erlotinib HCl (Selvanayagam *et al.*, 2008). ‡ Erlotinib–EGFR kinase complex (Stamos *et al.*, 2002). § Only one disordered component.

Table 2
Hydrogen-bond and short-contact geometry (Å, °) for (I).

D—H···A	D—H	H···A	D···A	D—H···A
N3—H3*N*···O1*W*	0.836 (16)	2.290 (17)	3.1123 (18)	167.9 (14)
O1*W*—H1*W*···O3^{i}	0.80 (2)	2.30 (2)	3.0485 (18)	156 (2)
O1*W*—H2*W*···N1^{ii}	0.85 (2)	2.03 (2)	2.8742 (18)	173 (2)
C4—H4···O1*W*	0.93	2.33	3.248 (2)	171
C16—H16···N2	0.93	2.27	2.874 (2)	122
C20—H20···O1*W*	0.93	2.50	3.323 (2)	148
C12—H12*B*···*Cg*2^{iii}	0.97	2.76	3.642 (2)	151

Symmetry codes: (i) $-x+2, -y+1, -z+2$; (ii) $x+1, y, z$; (iii) $-x+1, -y+1, -z+2$.

Table 3
Hydrogen-bond and short-contact geometry (Å, °) for (II).

D—H···A	D—H	H···A	D···A	D—H···A
N1—H1*N*···O6	0.98 (3)	1.68 (3)	2.633 (3)	163 (3)
N3—H3*N*···O5^{i}	0.88 (3)	1.94 (3)	2.783 (3)	160 (2)
C4—H4···O5^{i}	0.93	2.29	3.087 (3)	144
C16—H16···N2	0.93	2.29	2.885 (3)	121
C20—H20···O5^{i}	0.93	2.57	3.225 (3)	128
C12—H12*B*···*Cg*3^{ii}	0.97	2.77	3.907 (3)	160

Symmetry codes: (i) $x, y-1, z$; (ii) $-x, -y+1, -z+1$.

Data collection

Bruker SMART APEX CCD area-detector diffractometer
10367 measured reflections
3758 independent reflections
2996 reflections with $I > 2\sigma(I)$
$R_{int} = 0.032$

Refinement

$R[F^2 > 2\sigma(F^2)] = 0.067$
$wR(F^2) = 0.142$
$S = 1.17$
3758 reflections
299 parameters
H atoms treated by a mixture of independent and constrained refinement
$\Delta\rho_{max} = 0.25$ e Å^{-3}
$\Delta\rho_{min} = -0.18$ e Å^{-3}

Compound (III)

Crystal data

$C_{22}H_{23}N_3O_4\cdot0.5C_4H_4O_4\cdot2H_2O$
$M_r = 487.50$
Triclinic, $P\overline{1}$
$a = 7.967$ (2) Å
$b = 13.248$ (4) Å
$c = 13.745$ (4) Å
$\alpha = 108.916$ (5)°
$\beta = 106.673$ (5)°
$\gamma = 101.909$ (5)°
$V = 1240.9$ (6) Å^3
$Z = 2$
Mo $K\alpha$ radiation
$\mu = 0.10$ mm^{-1}
$T = 294$ K
0.18 × 0.16 × 0.11 mm

Data collection

Bruker SMART APEX CCD area-detector diffractometer
12036 measured reflections
4364 independent reflections
3501 reflections with $I > 2\sigma(I)$
$R_{int} = 0.023$

Refinement

$R[F^2 > 2\sigma(F^2)] = 0.054$
$wR(F^2) = 0.140$
$S = 1.08$
4364 reflections
379 parameters
56 restraints
H atoms treated by a mixture of independent and constrained refinement
$\Delta\rho_{max} = 0.27$ e Å^{-3}
$\Delta\rho_{min} = -0.15$ e Å^{-3}

All the N-bound H atoms of the erlotinib molecules [(I), (II) and (III)] were located in difference Fourier maps and their positions and isotropic displacement parameters were refined. The water H atoms of (I) and (III) were located in difference Fourier maps and their positions were refined. The isotropic displacement parameters of the water H atoms were fixed at 1.2 times the U_{eq} values of their parent O atoms. All other H atoms were located in a difference density map, positioned geometrically and included as riding atoms, with C—H = 0.93–0.98 Å and U_{iso}(H) = 1.2U_{eq}(C). The site-occupancy factors of disordered atoms C13/O2/C14 of (I) refined to 0.554 (7) and 0.446 (7). The geometries about the disordered atoms were restrained with C12—C13 = C12—C131 = 1.52 (1) Å and C13—O2 = C131—O21 = O2—C14 = O21—C141 = 1.42 (1) Å. Atom C11 of (I) shows a large displacement parameter and the anisotropic displacement parameters of atoms C10/O4/C11 were restrained to be similar [SIMU instruction in *SHELXL97* (Sheldrick, 2008)]; the direction of motion along the axis between these atoms was also restrained (DELU instruction in *SHELXL97*). In (III), atoms O5/O6/C23/C24 of the hemifumaric acid molecule were disordered over two sites (O5/O6/C23/C24 and O51/O61/C231/C241) and the site-occupation factors refined to 0.55 (2) and 0.45 (2). The anisotropic displacement parameters of the major and minor components were restrained to be similar (SIMU instruction in *SHELXL97*), and the direction of motion along the axis between these atoms was also restrained (DELU instruction in *SHELXL97*). Distance restraints were also applied to the disordered components. The O-bound H atom of the fumaric acid was located in difference Fourier maps and found to be shared by disordered atoms O5 and O51. The positions and isotropic displacement parameter were refined. The methyl groups were allowed to rotate but not to tip.

Table 4
Hydrogen-bond and short-contact geometry (Å, °) for (III).

D—H···A	D—H	H···A	D···A	D—H···A
N3—H3*N*···O2*W*	0.83 (2)	2.22 (2)	2.993 (3)	155 (2)
O5—H5*O*···N1	0.96 (4)	1.60 (4)	2.560 (3)	166 (4)
O1*W*—H1*W*···O2	0.83 (4)	2.10 (4)	2.884 (3)	157 (3)
O1*W*—H2*W*···O4	0.85 (4)	2.14 (4)	2.956 (3)	161 (4)
O2*W*—H3*W*···O1*W*^{i}	0.83 (4)	1.99 (4)	2.819 (3)	175 (3)
O2*W*—H4*W*···O6^{ii}	0.86 (5)	2.03 (6)	2.889 (17)	176 (5)
C9—H9*A*···O1*W*^{i}	0.97	2.59	3.436 (4)	146
C20—H20···N2	0.93	2.33	2.863 (4)	116
C22—H22···O1*W*^{ii}	0.93	2.54	3.444 (4)	164
C12—H12*A*···*Cg*3^{iii}	0.97	2.76	3.642 (2)	151

Symmetry codes: (i) $-x, -y+1, -z$; (ii) $-x+1, -y+1, -z+1$; (iii) $-x+1, -y+1, -z+2$.

For all compounds, data collection: *SMART* (Bruker, 2001); cell refinement: *SAINT* (Bruker, 2001); data reduction: *SAINT*; program(s) used to solve structure: *SHELXS97* (Sheldrick, 2008); program(s) used to refine structure: *SHELXL97* (Sheldrick, 2008); molecular graphics: *DIAMOND* (Brandenburg & Putz, 2005); software used to prepare material for publication: *SHELXL97*.

The authors thank Dr J. S. Yadav, Director, IICT, Hyderabad, for his kind encouragement.

Supplementary data for this paper are available from the IUCr electronic archives (Reference: SF3120). Services for accessing these data are described at the back of the journal.

References

Berman, H. M., Westbrook, J., Feng, Z., Gilliland, G., Bhat, T. N., Weissig, H., Shindyalow, I. N. & Bourne, P. E. (2000). *Nucleic Acids Res.* **28**, 235–242.

Bernstein, J., Davis, R. E., Shimoni, L. & Chang, N.-L. (1995). *Angew. Chem. Int. Ed. Engl.* **34**, 1555–1573.
Brandenburg, K. & Putz, H. (2005). *DIAMOND*. Release 3.0c. Crystal Impact GbR, Bonn, Germany.
Bruker (2001). *SAINT* (Version 6.28a) and *SMART* (Version 5.625). Bruker AXS Inc., Madison, Wisconsin, USA.
Desiraju, G. R. & Steiner, T. (1999). *The Weak Hydrogen Bond in Structural Chemistry and Biology*. Oxford University Press.
Etter, M. C. (1990). *Acc. Chem. Res.* **23**, 120–126.
Etter, M. C., MacDonald, J. C. & Bernstein, J. (1990). *Acta Cryst.* B**46**, 256–262.
Ghosh, S., Jennissen, J. D., Liu, X.-P. & Uckun, F. M. (2001). *Acta Cryst.* C**57**, 76–78.
Glusker, J. P. (1998). *Topics in Current Chemistry*, Vol. 198, pp. 1–56. Heidelberg: Springer-Verlag.
Rusch, V., Mendelsohn, J. & Dmitrovsky, E. (1996). *Cytokine Growth Factor Rev.* **7**, 133–141.
Selvanayagam, S., Sridhar, B. & Ravikumar, K. (2008). *Acta Cryst.* E**64**, o931.
Sheldrick, G. M. (2008). *Acta Cryst.* A**64**, 112–122.
Stahly, G. P. (2007). *Cryst. Growth Des.* **7**, 1007–1026.
Stamos, J., Sliwkowski, M. X. & Eigenbrot, C. (2002). *J. Biol. Chem.* **277**, 46265–46272.
Xia, M. (2005). *Acta Cryst.* E**61**, o3380–o3382.
Yarden, Y. & Ullrich, A. (1988). *Annu. Rev. Biochem.* **57**, 443–478.